5-1-2004

Comparison of Near-Field Millimeter Wave Probes for Detecting Corrosion Pit under Paint

Mohammad Tayeb Ahmad Ghasr
Missouri University of Science and Technology, mtg7w6@mst.edu

Sergey Kharkovsky
Missouri University of Science and Technology

R. Zoughi
Missouri University of Science and Technology, zoughi@mst.edu

Russell A. Austin

Recommended Citation

M. T. Ghasr et al., "Comparison of Near-Field Millimeter Wave Probes for Detecting Corrosion Pit under Paint," *Proceedings of the 21st IEEE Instrumentation and Measurement Technology Conference (2004, Como, Italy)*, vol. 3, pp. 2240-2244, Institute of Electrical and Electronics Engineers (IEEE), May 2004.
The definitive version is available at https://doi.org/10.1109/IMTC.2004.1351537

IMTC 2004 – Instrumentation and Measurement
Technology Conference
Como, Italy, 18-20 May 2004

Comparison of Near-Field Millimeter Wave Probes for Detecting Corrosion Pit under Paint

M. Ghasr[1], S. Kharkovsky[1], R. Zoughi[1] and R. Austin[2]
[1]Applied Microwave Nondestructive Testing Laboratory (*amntl*)
Electrical and Computer Engineering Department
University of Missouri-Rolla
Rolla, MO 65409

[2]Texas Research Institute at Austin (TRI-Austin)
9063 Bee Caves Road
Austin, TX 78733-6201

Abstract *- Corrosion pitting detection is a critical issue in the maintenance of aircraft. Near-field microwave nondestructive techniques have been successfully used for detection of corrosion under paint. In this paper a comparison between several different millimeter wave probes is made for the detection and evaluation of corrosion precursor pitting under paint at Ka-band and V-band. Since the pittings investigated here are very small in size, spatial resolution and sensitivity of the probes are critical issues. It is shown that modified open-ended rectangular probes namely, tapered waveguide and dielectric slab-loaded waveguide probes provide high resolution and sensitivity for the detection and evaluation of very small pittings under paint.*

I. INTRODUCTION

Critical aircraft structural components, such as wings and fuselages, are exposed to harsh environments that vary considerably in temperature and moisture content. These varied environmental conditions lead to corrosion of these components. In most cases the corrosion is hidden under paint and primer and cannot be visually detected. Thus, detection is only possible when corrosion becomes severe and causes blistering of the paint. When this happens a relatively large area must be rehabilitated which may require significant time, resources and downtime of the aircraft. The initiation of corrosion is preceded by the presence of corrosion precursor pitting. Detection of precursor pitting yields information about the susceptibility to corrosion initiation [1-3]. The size (area and depth) of a precursor pitting is very small (fractions of a millimeter), otherwise when it becomes relatively large corrosion process has already initiated. Therefore, nondestructive detection of corrosion pitting is an important practical concern in aircraft industry.

The small size of a pitting (in the tens of micrometer range) and the fact that it is covered by paint and primer limits the number of nondestructive methods that can be used to detect and evaluate it. Near-field microwave nondestructive testing (NDT) techniques, utilizing open-ended rectangular waveguide probes, have been successfully used to detect the presence of corrosion product under paint and primer in both steel and aluminum substrates [4-6]. In addition, near-field microwave NDT methods have been successful in detecting precursor pitting under paint [7]. Near-field microwave NDT techniques have also been used to detect surface anomalies in metallic structures, such as scratches, cracks, pitting and dents [8-12]. Microwave signals are capable of penetrating paint and primer and interact with surface anomalies, and measurements can be made in a one-sided and non-contact fashion.

II. APPROACH

When using near-field microwave NDT methods spatial resolution is primarily determined by the probe (i.e., an open-ended rectangular waveguide) dimensions. This is an important feature of these NDT methods. However, the detection of precursor pitting may require higher resolution probes than just open-ended rectangular waveguide probes.

At a selected operating frequency band, reducing the probe aperture dimensions results in higher spatial resolution. One of the methods used to obtain higher spatial resolution involves tapering a rectangular waveguide probe [7]. Another possible method to increase spatial resolution is to electrically reduce the size of the probe by changing the distribution of the electric field in the waveguide. These two methods may be used together to further increase the spatial resolution. However, decreasing the size of the probe aperture adversely affects its radiation efficiency. Radiation efficiency is important for practical scanning environment where the probe should be at a relatively large distance to the pittings and also to be able to detect them through coatings such as paint. A compromise should be reached between increasing the spatial resolution and decreasing the radiation efficiency (sensitivity) of a given probe.

0-7803-8248-X/04/$17.00 ©2004 IEEE

Consequently, several open-ended probes were designed and developed for this purpose at Ka-band (26.5-40 GHz) and V-band (50-75 GHz). These open-ended probes included a rectangular waveguide, single and double-tapered rectangular waveguides, and dielectric slab-loaded waveguides (several different dielectric slab geometries). A phase sensitive reflectometer was used to detect and evaluate the relative spatial resolution and sensitivity of these probes for detecting small pittings.

III. RESULTS

A. Field Distribution

As mentioned above, changing the distribution of the electric field in a waveguide probe may affect its resolution. In a dielectric slab-loaded waveguide, the electric field tends to concentrate in the slab [13-15]. To optimize this type of waveguides for the purpose of pit imaging, the performance of the dielectric slab-loaded waveguide were investigated numerically for slab location, thickness, and permittivity.

Figure 1 shows the calculated electric field distribution of the TE_{10} mode in a Ka-band rectangular waveguide (WR-28) loaded with a 1 mm-thick slab of a dielectric material (in the center of the waveguide broad dimension) for four different relative permittivity values of: 1) $\varepsilon'_r = 1$ (no dielectric slab), 2) $\varepsilon'_r = 2.5$, 3) $\varepsilon'_r = 4$ and 4) $\varepsilon'_r = 9.8$. The results show that as the permittivity of the dielectric slab increases the electric field becomes more concentrated within the dielectric slab and hence produces a waveguide aperture with higher spatial resolution when used for near-field imaging.

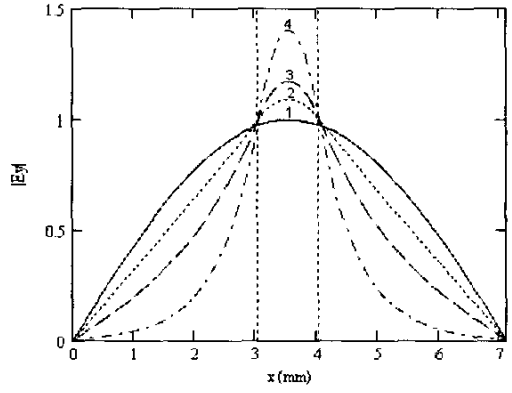

Fig 1: Electric field distribution in a rectangular waveguide loaded with a 1 mm-thick dielectric slab having various permittivies at 35 GHz.

As it is shown in Figure 1, a vertical dielectric slab in the middle of the waveguide localizes the electric field inside and around the slab. The extent of this spatial localization depends on the dielectric permittivity of the dielectric slab and its width. Figure 2 shows the normalized electric field distribution in a dielectric slab-loaded rectangular waveguide for a dielectric slab of permittivity $\varepsilon'_r = 9.8$ and normalized width of c/a = 0.05, 0.15, and 0.3. In Figure 2, c is the width of the dielectric slab, and d is the extent of effective electric field intensity localization at selected level of $|Ey| / |Ey|_{max} = 0.5$. It can be seen from Figure 2 that at selected effective level of normalized electric field intensity $|Ey| / |Ey|_{max} = 0.5$, d/a depends on the slab width non-monotonically.

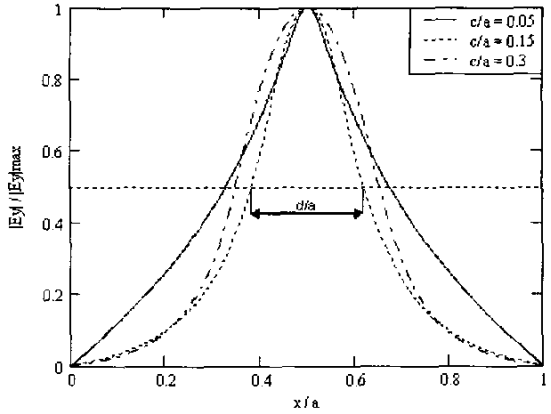

Fig 2: Normalized electric field intensity distribution in a rectangular waveguide loaded with a dielectric slab with permittivity of $\varepsilon'_r = 9.8$ for different normalized slab width c/a.

Figure 3 shows the extent of normalized effective electric field (TE_{10} mode) intensity localization as a function of the width of the dielectric slab for a dielectric permittivity of: 1) $\varepsilon'_r = 2.5$, 2) $\varepsilon'_r = 4$, 3) $\varepsilon'_r = 9.8$ and 4) $\varepsilon'_r = 15$.

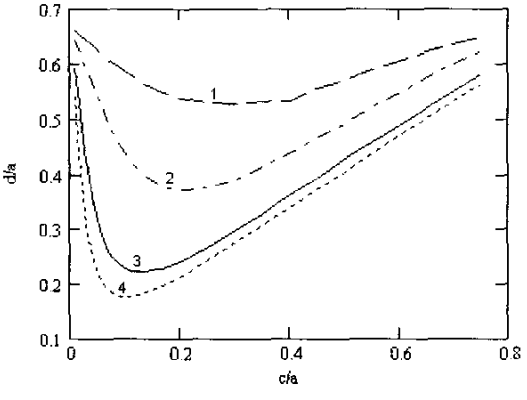

Fig 3: The extent of normalized effective electric field localization, d/a, vs. normalized slab width (c/a) for different dielectric permittivity of the slab.

It can be seen from Figure 3 that for each dielectric permittivity, there is an optimum slab width providing the

smallest effective extent of electric field localization which corresponds to the highest concentration of the electric field inside and near the slab. For example for a dielectric permittivity of 9.8, a relative slab width of 0.13 gives maximum localization of TE_{10} electric field at the electric field intensity level of $0.5|Ey|_{max}$.

B. Imaging

Microwave and millimeter wave images of pittings can be obtained by raster scanning an area that may contain a pitting. In this way an intensity image proportional to the phase or magnitude of reflection coefficient at the aperture of the probe can be obtained. A pitting with a diameter and a depth of approximately 1 millimeter was scanned using four probes at Ka-band. The probes were: an open-ended rectangular waveguide (aperture dimensions 7.11 mm x 3.56 mm), a dielectric slab-loaded (with permittivity of ε'_r = 9.8, c/a = 0.14 mm) rectangular waveguide (aperture dimensions 7.11 mm x 3.56 mm), a double tapered waveguide (aperture dimensions 4.8 mm x 2.4 mm), and a single tapered waveguide (aperture dimensions 7.11 mm x 0.5 mm). The resulting images are shown in Figures 4-7.

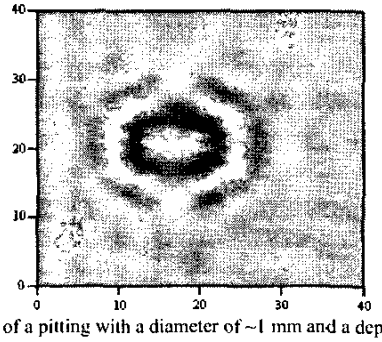

Fig 4: Image of a pitting with a diameter of ~1 mm and a depth of ~1 mm using an open-ended rectangular waveguide at Ka-band.

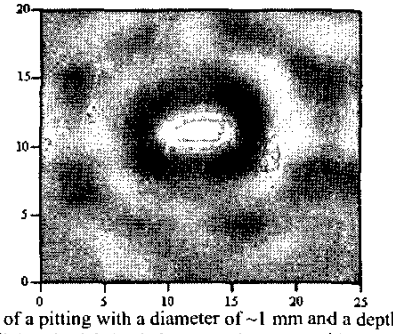

Fig 5: Image of a pitting with a diameter of ~1 mm and a depth of ~1 mm using a dielectric slab-loaded rectangular waveguide at Ka-band.

It can be observed from Figures 4-7 that each probe produced an image for the pitting with a unique shape and features. Figure 4 shows that the open-ended rectangular waveguide probe produced a double image of the pitting. This is because the pitting is small compared to the aperture of the probe and thus the pit interacts with the edges of the aperture. At higher standoff distances, the open-ended rectangular waveguide produces one spot as an indication for the pit. In Figure 5 the pitting shows as one spot in the image, since the electric field is concentrated in the dielectric slab in the middle of the waveguide. In Figure 6 the pitting shows also as one spot due to the relatively smaller size for the probe. In Figure 7, the size and shape of the image approaches the shape of the pitting due to the small open aperture size of the probe.

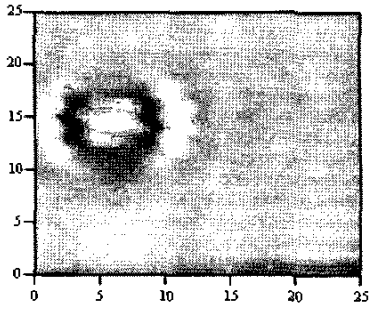

Fig 6: Image of a pitting with a diameter of ~1 mm and a depth of ~1 mm using a double tapered waveguide at Ka-band.

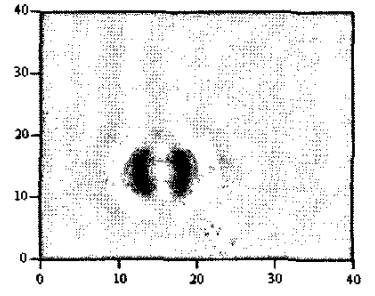

Fig 7: Image of a pitting with a diameter of ~1 mm and a depth of ~1 mm using a single tapered waveguide at Ka-band.

Each image in Figures 4-7 also shows rings around the image of the pitting as a result of wave propagation between the flange and the sample. The presence of rings increases the probability of pit detection. Also it is worth noting in Figure 5 that the dielectric slab reduced the intensity of the rings, as expected (i.e., the electric field is concentrated at the center of the probe).

The spot intensity in each image depends on the radiation efficiency of the probe. The images of Figures 4-7 are normalized therefore it is not possible to compare the difference in intensity between the images. However, when these images were augmented together before normalization (not shown in this paper), we observed that the double tapered and the dielectric slab-loaded waveguides produce images with higher intensity than the

open-ended waveguide and the tapered waveguide. This is due to the relatively small physical aperture dimension compared to the size of the pit and large electrical aperture dimension.

Increasing the spatial resolution of the probe by decreasing its electrical size, results in a decrease in its radiation efficiency. Therefore, in order to obtain images of very small pits, the measurement should be performed at a very small standoff distance. However, for small standoff distances the probe is very sensitive to variation in standoff distance. This is because of the perturbation on the near-field evanescence fields.

At Ka-band, only the single tapered probe could detect exposed machined pits of 500 micrometer-diameter and depth as small as 150 micrometers. Figure 8 shows the image of 500 micrometer-diameter pits each with a depth of (from left to right) 150, 200, and 500 micrometers. In this image the difference in the intensity of the indications represent the variation in depth.

The original image was masked by the signal due to standoff distance variation. Therefore, the image was processed to remove standoff distance variation effect. At the bottom left corner of the image in Figure 8 an indication may be observed. This indication is leftover from the signal due to the standoff distance variation that was not removed totally and it does not show any features of the pit namely, the spots and rings.

In order to increase both the spatial resolution and radiation efficiency, the frequency of operation may be increased. At high frequencies the probe has high spatial resolution due to the small aperture size and good radiation efficiency due to a relatively large electrical size. This was investigated on probes operating at V-band. Figure 9 shows the image of 500 micrometer-diameter and 150 micrometer-depth pit under paint obtained using an open-ended rectangular waveguide at V-band (aperture dimensions of 3.8 mm x 1.9 mm). Figure 10 shows an image for the same pit using a dual tapered waveguide with aperture dimensions of 2.54 mm x 1.27 mm.

Comparing the images in Figures 9 and 10 we can observe that the dual tapered probe with smaller aperture size gave a better contrast than the image obtained by the open-ended rectangular waveguide. On the other hand, in Figure 9, due to the higher radiation efficiency, the probe produced three times the number of rings around the pitting indication compared to the other probe. This is advantageous since it increase the probability of detecting the pit.

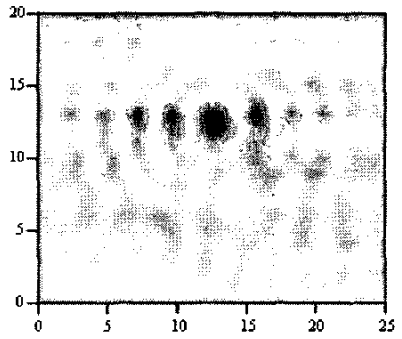

Fig 9: Image of a pitting of 150 micrometer-depth and 500 micrometer-diameter under paint obtained using a V-band open-ended rectangular waveguide probe.

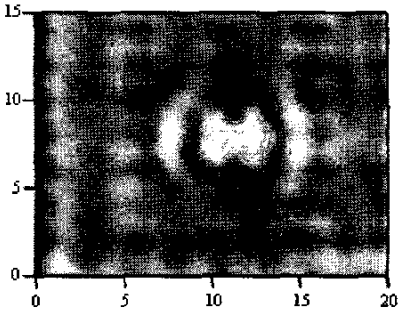

Fig 10: Image of a pitting of 150 micrometer-depth and 500 micrometer-diameter under paint obtained using a double tapered waveguide probe at V-band.

The V-band dual tapered probes could detect pits of dimension down to a diameter of 200 micrometers and depth of 500 micrometers under paint and appliqué and

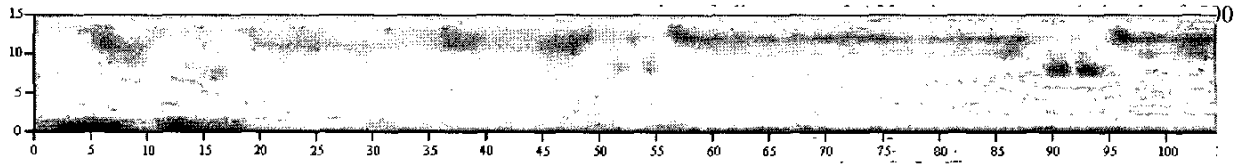

Fig 8: Image of three pits of 500 micrometer-diameter and depth of (from left to right) 150, 200, and 500 micrometers, obtained using the tapered probe at Ka-band.

One of the issues that need to be overcome is the effect of standoff distance (distance between the waveguide probe and the metal surface under test) variation on the results. High resolution probes are sensitive to standoff distance variation, which may mask the indication of a pitting. Further processing may be required to "clean" such images and extract the indication of pitting.

IV. CONCLUSION

Different types of near-field millimeter wave probes for detection and evaluation of pitting under paint using raster scanning were investigated and compared. The probes investigated produced images of a pit which depend on the type of the probe, operating frequency and standoff distance. At selected frequency bands, various pit dimensions, and range of standoff distances, the open-ended waveguide probe produced a double image of the pit as a signature of the probe and distinct rings around the image as a signature of the probe flange. This kind of images may provide high probability of detection, but for the evaluation of pitting, an image similar to the real shape of the pit is more desirable. A single image of the investigated pit was obtained by a dielectric slab-loaded waveguide and tapered waveguide probes. It was shown that a significant increase in the electric field concentration may be obtained in a dielectric slab-loaded waveguide.

The dielectric slab-loaded waveguide probe demonstrated the highest sensitivity and good resolution, which increased with the increase in the operating frequency. The tapered waveguide demonstrated the highest resolution among all probes, but its sensitivity was lower than the dielectric slab-loaded waveguide probe.

For measurements conducted in this investigation, dielectric slab-loaded waveguide probe at V-band may provide optimal combination of spatial resolution and sensitivity for the detection and evaluation of pitting under paint. The tapered waveguide probe may be also useful for pit detection and evaluation in cases of small standoff distances such as when scanning exposed metal surfaces.

ACKNOWLEDGMENT

The funding for this research has been provided through an Air Force Phase II SBIR grant.

REFERENCES

[1]. "Corrosion Tests and Standards: Application and Interpretation", edited by Robert Baboian, American Society for Testing and Materials, Philadelphia, PA, 1995.

[2]. Funke, W., "Blistering of Paint Films" in Corrosion Control by Organic Coatings, Edited by Henry Leidheiser, Jr., National Association of Corrosion Engineers, Houston, TX, pp. 97-102, 1981.

[3]. Collins, J.A., "Failure of Materials in Mechanical Design" 2nd edition, Wiley Interscience, New York, NY, 1993.

[4]. Qaddoumi, N., A. Shroyer and R. Zoughi, "Microwave Detection of Rust Under Paint and Composite Laminates," *Research in Nondestructive Evaluation*, vol. 9, no. 4, pp. 201-212, 1997.

[5]. Qaddoumi, N., L. Handjojo, T. Bigelow, J. Easter, A. Bray and R. Zoughi, "Microwave Corrosion Detection Using Open-Ended Rectangular Waveguide Sensors," *Materials Evaluation*, vol. 58, no. 2, pp. 178-184, February 2000.

[6]. Hughes, D., N. Wang, T. Case, K. Donnell, R. Zoughi, R. Austin and M. Novack "Microwave Nondestructive Detection of Corrosion Under Thin Paint and Primer in Aluminum Panels," *Special Issue of Subsurface Sensing Technologies and Applications: on Advances and Applications in Microwave and Millimeter Wave Nondestructive Evaluation*, vol. 2, no. 4, pp. 435-451, 2001.

[7]. Hughes, D., R. Zoughi, R. Austin, N. Wood and R. Engelbart, "Near-Field Microwave Detection of Corrosion Precursor Pitting under Thin Dielectric Coatings in Metallic Substrates," *Proceedings of the Twenty-ninth Annual Review of Progress in Quantitative Nondestructive Evaluation*, vol. 22B, pp. 462-469, Bellingham, WA, July 14-19, 2002.

[8]. Zoughi, R., C. Huber, S. Ganchev, R. Mirshahi, V. Otashevich, E. Ranu and T. Johnson, "Rolled Steel Surface Inspection Using Microwave Methods," *Proceedings of the Eighth International Symposium on Nondestructive Characterization of Materials*, vol. VIII, pp. 285-290, Boulder, CO, June 15-20, 1997.

[9]. Yeh, C. and R. Zoughi, "A Novel Microwave Method for Detection of Long Surface Cracks in Metals," *IEEE Transactions on Instrumentation and Measurement*, vol. 43, no. 5, pp. 719-725, October, 1994.

[10]. Huber, C., H. Abiri, S. Ganchev and R. Zoughi, "Analysis of the Crack Characteristic Signal Using a Generalized Scattering Matrix Representation," *IEEE Transactions on Microwave Theory and Technique*, vol. 45, no. 4, pp. 477-484, April, 1997.

[11]. Huber, C., H. Abiri, S. Ganchev and R. Zoughi, "Modeling of Surface Hairline Crack Detection in Metals Under Coatings Using Open-Ended Rectangular Waveguides," *IEEE Transactions on Microwave Theory and Techniques*, vol. 45, no. 11, pp. 2049-2057, November 1997.

[12]. Zoughi, R., C. Huber, N. Qaddoumi, E. Ranu, V. Otashevich, R. Mirshahi, S. Ganchev and T. Johnson, "Real-Time and On-Line Microwave Inspection of Surface Defects in Rolled Steel," *Proceedings of the Asia-Pacific Microwave Conference, APMC'97*, Hong Kong, pp. 1081-1084, December 2-5, 1997.

[13]. Outifa, L. M. Delmotte and H. Jullien, "Dielectric and Geometric Dependence of Electric Filed and Power Distribution in a Waveguide Heterogeneously Filled with Lossy Dielectrics," *IEEE Transactions on Microwave Theory and Technique*, vol. 45, no. 8, pp. 1154-1161, August 1997.

[14]. Eberhardt N. "Propagation in the Off Center E-Plane Dielectric Loaded Waveguide" *IEEE Transactions on Microwave Theory and Technique*, vol. MTT-15, no. 5, pp. 282-289, May 1967.

[15]. Vartanian, P. W. Ayres and A. Helgesson, "Propagation in Dielectric Slab Loaded Rectangular Waveguide" IEEE *Transactions on Microwave Theory and Technique*, vol. 6, no. 2, pp.215-222, April, 1958.